



香港城市大學
City University of Hong Kong

專業 創新 胸懷全球
Professional · Creative
For The World

CityU Scholars

A low dimensional approach on network characterization

Li, Benjamin Y. S.; Zhan, Choujun; Yeung, Lam F.; Ko, King T.; Yang, Genke

Published in:
PLoS ONE

Published: 16/10/2014

Document Version:
Final Published version, also known as Publisher's PDF, Publisher's Final version or Version of Record

License:
CC BY

Publication record in CityU Scholars:
[Go to record](#)

Published version (DOI):
[10.1371/journal.pone.0109383](https://doi.org/10.1371/journal.pone.0109383)

Publication details:
Li, B. Y. S., Zhan, C., Yeung, L. F., Ko, K. T., & Yang, G. (2014). A low dimensional approach on network characterization. *PLoS ONE*, 9(10), [e109383]. <https://doi.org/10.1371/journal.pone.0109383>

Citing this paper

Please note that where the full-text provided on CityU Scholars is the Post-print version (also known as Accepted Author Manuscript, Peer-reviewed or Author Final version), it may differ from the Final Published version. When citing, ensure that you check and use the publisher's definitive version for pagination and other details.

General rights

Copyright for the publications made accessible via the CityU Scholars portal is retained by the author(s) and/or other copyright owners and it is a condition of accessing these publications that users recognise and abide by the legal requirements associated with these rights. Users may not further distribute the material or use it for any profit-making activity or commercial gain.

Publisher permission

Permission for previously published items are in accordance with publisher's copyright policies sourced from the SHERPA RoMEO database. Links to full text versions (either Published or Post-print) are only available if corresponding publishers allow open access.

Take down policy

Contact lbscholars@cityu.edu.hk if you believe that this document breaches copyright and provide us with details. We will remove access to the work immediately and investigate your claim.



A Low Dimensional Approach on Network Characterization

Benjamin Y. S. Li^{1*}, Choujun Zhan², Lam F. Yeung¹, King T. Ko¹, Genke Yang³

1 Department of Electronic Engineering, City University of Hong Kong, Hong Kong, Hong Kong, **2** Department of Electronic and Information Engineering, The Hong Kong Polytechnic University, Hong Kong, Hong Kong, **3** Department of Automation, Shanghai Jiao Tong University, Shanghai, China

Abstract

In many applications, one may need to characterize a given network among a large set of base networks, and these networks are large in size and diverse in structure over the search space. In addition, the characterization algorithms are required to have low volatility and with a small circle of uncertainty. For large datasets, these algorithms are computationally intensive and inefficient. However, under the context of network mining, a major concern of some applications is speed. Hence, we are motivated to develop a fast characterization algorithm, which can be used to quickly construct a graph space for analysis purpose. Our approach is to transform a network characterization measure, commonly formulated based on similarity matrices, into simple vector form signatures. We shall show that the $N \times N$ similarity matrix can be represented by a dyadic product of two N -dimensional signature vectors; thus the network alignment process, which is usually solved as an assignment problem, can be reduced into a simple alignment problem based on separate signature vectors.

Citation: Li BYS, Zhan C, Yeung LF, Ko KT, Yang G (2014) A Low Dimensional Approach on Network Characterization. PLoS ONE 9(10): e109383. doi:10.1371/journal.pone.0109383

Editor: Vince Grolmusz, Mathematical Institute, Hungary

Received: April 7, 2014; **Accepted:** September 2, 2014; **Published:** October 16, 2014

Copyright: © 2014 Li et al. This is an open-access article distributed under the terms of the Creative Commons Attribution License, which permits unrestricted use, distribution, and reproduction in any medium, provided the original author and source are credited.

Data Availability: The authors confirm that all data underlying the findings are fully available without restriction. Data are from the following studies: Uetz, P., Dong, Y. A., Zeretzke, C., Atzler, C., Baiker, A., Berger, B.,... & Haas, J. (2006). Herpesviral protein networks and their interaction with the human proteome. *Science*, 311(5758), 239-242. Fossum, E., Friedel, C. C., Rajagopala, S. V., Titz, B., Baiker, A., Schmidt, T.,... & Haas, J. (2009). Evolutionarily conserved herpesviral protein interaction networks. *PLoS pathogens*, 5(9), e1000570. All relevant data from this study are within the paper and its Supporting Information files.

Funding: This project is supported by CityU Strategic Research Grant 7003016. <http://www.cityu.edu.hk/ro/dlSRG.htm>. The funders had no role in study design, data collection and analysis, decision to publish, or preparation of the manuscript.

Competing Interests: The authors have declared that no competing interests exist.

* Email: yeelsi2-c@my.cityu.edu.hk

Introduction

In recent years, network mining has received a considerable amount of attentions. One important aspect of network mining is to measure the dissimilarities among networks since they can provide information to reproduce a graph space and allow analysis to be performed [1,2]. Yet due to the complex nature of networks, this is considered to be a challenging task [1–4].

Although it is challenging, many algorithms have been developed to solve the network comparison problem. Umeyama formulated the problem into a combinatorial optimization problem and was solved via eigendecomposition [5], Singh et al. proposed a Page rank like similarity matrix IsoRank and employed it on the search of optimal assignment [6], Li et al. proposed an integer quadratic programming approach and was solved using an ellipsoid trust region method with interior point technique [7], etc. These methods mainly consider a one-to-one comparison and may not be efficient to handle large data set. Signature extraction is one effective way to treat such large volume of data. While representing the data with a signature vector, the comparison among complex objects can be reduced to comparison between signature vectors. In addition, for pairwise comparisons, the aforementioned optimization problem is no longer required to be solved in every pairs of networks. A typical type of signature vector is the motif count vector, which summarizes the network structures by the occurrence frequencies of specific subgraphs [8–12].

Although many effective algorithms are being designed for motif counting, the computational demand is still high and the computation complexity increases as more motifs are considered.

In this paper, an alternative approach with a balance between precision and computational efficiency is proposed. Eigenvector signature distance (EVSD) is a dissimilarity measure for large-scale pairwise network comparison based on signature vector extraction techniques. The basic idea of EVSD is to represent a network by a signature vector, which is the Perron-Frobenius (PF) vector of a network's adjacency matrix. In this paper we shall show that the network comparison and alignment problem can be reduced from a matrix alignment problem into a vector alignment problem. Consequently, this vector alignment problem can be solved by simple sorting operations. Hence the complexity is reduced from $O(N^4)$ to $O(N \log N)$.

The optimal distance EVSD can be further reconstructed into an agreement measure, eigenvector signature agreement (EVSA), which can be used to quantify the similarity between two networks. The distribution of EVSA has been studied through pairwise comparisons of artificially generated networks. Results have shown that EVSAs of networks with similar structure are notably higher than EVSAs of networks with dissimilar structures. In addition, comparison between EVSA and another state-of-art signature induced similarity measures, Graphlet Degree Distribution Agreement (GDDA), will be given in Section 3.2.2. The comparison results show that classifications based on EVSA have

a relatively stable distribution, which can provide a more convincing and consistent inference.

Methods

In this section we first formulate the network comparison problem, and then we show how the problem can be reduced and solved via the decomposition of Blondel’s similarity matrix. Finally, based on the solution of this problem, we introduce Eigenvector Signature Distance and Eigenvector Signature Agreement to quantify networks’ dissimilarity and similarity respectively

2.1 Preliminary

A graph $G(V, E)$ consists of the vertices set V and the edges set E . The edges set is a collection of all edges, each edge can be represented in the form of (u, v) , where $u, v \in V$. A network can be quantified by a number of statistical measures. For instance, degree of node v_i , $deg(v_i)$, which is the total number of edges connected to node v_i . The average degree, $deg_{avg} = \frac{2e}{v}$, where $e = |E|$ and $v = |V|$ respectively. The graph density $\sigma = \frac{2e}{v(v-1)} = \frac{deg_{avg}}{v-1}$, is the ratio of the number of existing edges to the largest possible number of edges.

A graph G can also be represented by its adjacency matrix, $A = \{a_{ij}\} \in \mathbb{R}^{v \times v}$, entry $a_{ij} = 1$ shows that there is an edge connected from node i to node j , otherwise $a_{ij} = 0$. If the graph is undirected, the adjacency matrix will be symmetric. If the graph is connected, the adjacency matrix is irreducible.

2.2 Network Comparisons and Signature Vector

The network comparison problem can be considered as finding a graph distance metric d , which quantifies the difference between networks. There are many candidate measures that can be used [13–15]. Most of these measures need to deal with the problem caused by large amount of vertex mapping variations. For instance, if two networks of size 10 are being compared, then there exist 3628800 variations of vertex mapping. Computing the graph distance using the metric d on all the vertex mappings will be computationally demanding. Picking an arbitrary vertex mapping may yield a distance measure that is inappropriate for comparison.

An appropriate measure would be,

$$d(g, h) = \min_{Q \in \mathbb{P}} f(g, h, Q) \tag{1}$$

where g and h are graphs, $Q : V_g \rightarrow V_h$ is a mapping that maps nodes in graph g to h , \mathbb{P} is the set of all permutation matrices. f represents a metric that quantifies dissimilarity between g and h under the mapping Q . A practical formulation of (1) could be designed with the aid of a similarity matrix. Similarity matrix is a node based similarity measure which stores all node-to-node pairwise similarity information between two networks. With such matrix, the problem can be transformed into searching a suitable mapping of nodes between two networks, which at the same time maximize the sum of all node pair similarities. That is

$$P_0 : \max_{Q \in \mathbb{P}} trace(S(G, QHQ^T)) \tag{2}$$

where G and H are the adjacency matrices of graph g and h respectively. $S(G, H)$ is the similarity matrix which s_{ij} is the similarity between node i in network g and node j in network h .

Note that, there are more than one way to interpret similarity between two networks. In this paper we employed the similarity matrix proposed by Blondel et al. [16]. According to Blondel et al., the similarity matrix for graphs g and h with adjacency matrices G and H can be computed by the following iterative process.

$$Z_{k+1}(G, H) = \frac{HZ_kG^T + H^TZ_kG}{\|HZ_kG^T + H^TZ_kG\|_F} \tag{3}$$

where $\|\cdot\|_F$ is the Frobenius norm. Z_k will finally converge to the similarity matrix.

While g and h are undirected graphs, the iterative process can be simplified into

$$Z_{k+1} = \frac{HZ_kG}{\|HZ_kG\|_F} \tag{4}$$

Thus P_0 becomes

$$P_1 : \arg \max_{Q \in \mathbb{P}} trace(\lim_{k \rightarrow \infty} Z_k(G, QHQ^T)) \tag{5}$$

On the other hand, by multiplying Q^T to both side of the iterative process, we have

$$Q^TZ_{k+1}(G, QHQ^T) = \frac{HQ^TZ_kG}{\|HQ^TZ_kG\|_F} \tag{6}$$

Note that $\|HQ^TZ_kG\|_F = \|QHQ^TZ_kG\|_F$ as Frobenius norm is unitarily invariant.

Let $S_Q = \lim_{k \rightarrow \infty} Z_k(G, QHQ^T)$ and $S = \lim_{k \rightarrow \infty} Z_k(G, H)$, from (6) we have the following relationship

$$Q^TS_Q = S \tag{7}$$

Thus P_1 becomes

$$P_2 : \arg \max_{Q \in \mathbb{P}} trace(S_Q) = \arg \max_{Q \in \mathbb{P}} trace(QS) \tag{8}$$

P_2 is an $N \times N$ assignment problem which can be solved by the Hungarian method in $O(N^4)$ time. It is computational demanding for large N . The efficiency can be dramatically reduced by the following decomposition on the S matrix.

According to the well know Von Mises iteration method [17], the following iterative processes converge and $x = \lim_{k \rightarrow \infty} x_k$, $y = \lim_{k \rightarrow \infty} y_k$ are the Perron-Frobenius (PF) vectors of G and H respectively.

$$x_{k+1} = \frac{Gx_k}{\|Gx_k\|_2} \text{ and } y_{k+1} = \frac{Hy_k}{\|Hy_k\|_2} \tag{9}$$

Let y_k^Q be defined by $y_k = Q^T y_k^Q$. From (9) we have

$$y_{k+1}^Q = \frac{QHQ^T y_k^Q}{\|QHQ^T y_k^Q\|_2} \tag{10}$$

And we can see that y_k^Q is the PF vector of QHQ^T . Note that $\|QHQ^T y_{k+1}^Q\|_2 = \|HQ^T y_{k+1}\|_2$ as Euclidean norm is unitarily invariant.

Combining (9) and (10) we have

$$S_Q = Qy x^T \tag{11}$$

Thus P_2 becomes

$$P_3 : \arg \max_{Q \in \mathbb{P}} \text{trace}(Qy x^T) = \arg \max_{Q \in \mathbb{P}} x^T Qy \tag{12}$$

Since product of permutation matrices is still a permutation matrix, problem P_3 can be rewritten into the following form,

$$P_4 : \max_{Q_x, Q_y \in \mathbb{P}} x^T Q_x Q_y y \tag{13}$$

and the problem becomes finding optimal permutation on x and y such that their inner product is maximized. According to the rearrangement inequality [18], the inner product is maximized when the two vectors are sorting in descending order. That is,

$$P_5 : \max_{Q_x, Q_y \in \mathbb{P}} x^T Q_x Q_y y = \hat{x}^T \hat{y} \tag{14}$$

where $\hat{x}_i = x_{\Pi_x(i)}$ and $\hat{y}_i = y_{\Pi_y(i)}$, Π_x and Π_y are the optimal mapping such that

$$\hat{x}_1 \geq \dots \geq \hat{x}_N \text{ and } \hat{y}_1 \geq \dots \geq \hat{y}_N \tag{15}$$

Here \hat{x} and \hat{y} are considered as the eigenvector signatures (EVS) of the two networks. By combining equations (14) and (15), we can see that the original problem P_1 can be solved via a simple sorting algorithm with the aid of our proposed decomposition. Hence, once the eigenvector is computed, only $O(N \log N)$ time is needed to complete the alignment. When comparing with the case without the decomposition, the computational time of P_3 is reduced from $O(N^4)$ to $O(N \log N)$ on the alignment process. In addition, in the case of pairwise comparison among M networks, as signatures are only required to be compute and sorted once, thus the time complexity of our proposed method is only $O(MN \log N)$. Yet without the decomposition, an assignment problem is required to be solved in each comparison, hence the time complexity of the entire task is $O(M^2 N^4)$.

2.3 Eigenvector Signature Distance and Eigenvector Signature Agreement

The optimal value of P_0 can be shown to be related to the Euclidean distance between EVSs of two networks. The relation can be summarized by the following property.

Property 2.1 $\bar{c}(A_1, A_2) < \bar{c}(A_3, A_4)$ iff $\min_{Q \in \mathbb{P}} \|x_1 - Qx_2\|_2 > \min_{Q \in \mathbb{P}} \|x_3 - Qx_4\|_2$, where \mathbb{P} is the set of permutation matrices, A_1, \dots, A_4 are adjacency matrices and x_1, \dots, x_4 are their respective EVSs.

Proof of Property 2.1. Suppose $\bar{c}(A_1, A_2) < \bar{c}(A_3, A_4)$, we have

$$\max_{Q \in \mathbb{P}} x_1^T Qx_2 < \max_{Q \in \mathbb{P}} x_3^T Qx_4 \tag{16}$$

Hence

$$\min_{Q \in \mathbb{P}} \sqrt{2 - 2x_1^T Qx_2} > \min_{Q \in \mathbb{P}} \sqrt{2 - 2x_3^T Qx_4} \tag{17}$$

That is

$$\min_{Q \in \mathbb{P}} \|x_1 - Qx_2\|_2 > \min_{Q \in \mathbb{P}} \|x_3 - Qx_4\|_2 \tag{18}$$

On the other hand, if $\min_{Q \in \mathbb{P}} \|x_1 - Qx_2\|_2 > \min_{Q \in \mathbb{P}} \|x_3 - Qx_4\|_2$, we have

$$\min_{Q \in \mathbb{P}} \sqrt{2 - 2x_1^T Qx_2} > \min_{Q \in \mathbb{P}} \sqrt{2 - 2x_3^T Qx_4} \tag{19}$$

which is equivalent to

$$\min_{Q \in \mathbb{P}} 1 - x_1^T Qx_2 > \min_{Q \in \mathbb{P}} 1 - x_3^T Qx_4 \tag{20}$$

According to Perron-Frobenius Theorem, all entries of x_1, \dots, x_4 are nonnegatives, as Q is a permutation matrix so entries of Q should also be nonnegatives. Thus,

$$x_1 Qx_2 \geq 0 \text{ and } x_3^T Qx_4 \geq 0 \text{ for all } Q \in \mathbb{P} \tag{21}$$

Therefore

$$\max_{Q \in \mathbb{P}} x_1^T Qx_2 < \max_{Q \in \mathbb{P}} x_3^T Qx_4 \tag{22}$$

Hence,

$$\bar{c}(A_1, A_2) < \bar{c}(A_3, A_4) \tag{23}$$

According to the above property, for topological similar networks, the Euclidean distance between their corresponding EVSs will be smaller and vice versa. This indicates that the Euclidean distance between EVSs can be considered as the measure of dissimilarity between networks. With this, a network measure can be defined by:

$$d_{EVS}(g, h) \triangleq \frac{\|\hat{x} - \hat{y}\|_2}{\sqrt{2 - 2/\sqrt{N}}} \tag{24}$$

where g and h are graphs, \hat{x} and \hat{y} are their EVS respectively. The denominator $\sqrt{2-2/\sqrt{N}}$ is to normalize the measure so that $d_{EVS}(g,h) \in [0,1]$. This choice of value can be explained by the following property.

Property 2.2 *The farthest pair of vectors in the set $W = \{w|w \in \mathbb{R}^N, \|w\|_2 = 1, w_1 \geq \dots \geq w_N \geq 0\}$ are $[1,0,\dots,0]^T$ and $[1/\sqrt{N},\dots,1/\sqrt{N}]^T$.*

Proof of Property 2.2. Let $x = [1,0,\dots,0]^T$, $y = [1/\sqrt{N},\dots,1/\sqrt{N}]^T$ and $W = \{w|w \in \mathbb{R}^N, \|w\|_2 = 1, w_1 \geq \dots \geq w_N \geq 0\}$.

We show x and y are the farthest pair of vectors in the set W by contradiction.

Suppose x is not the farthest vector to y in the set W . There exists a vector $a \in W$ where

$$\|a-y\|_2 > \|x-y\|_2 \tag{25}$$

$$a^T y < x^T y \tag{26}$$

$$\sum_{i=1}^N \frac{a_i}{\sqrt{N}} < \frac{1}{\sqrt{N}} \tag{27}$$

$$\sum_{i=1}^N a_i < 1 \tag{28}$$

Since $0 \leq a_i \leq 1$

$$\sum_{i=1}^N a_i > \sum_{i=1}^N a_i^2 = 1 \tag{29}$$

which contradicts $a \in W$.

Suppose y is not the farthest vector to x in the set W . There exist a vector $b \in W$ where

$$\|x-b\|_2 > \|x-y\|_2 \tag{30}$$

$$x^T b < x^T y \tag{31}$$

$$b_1 < \frac{1}{\sqrt{N}} \tag{32}$$

Since $b_1 > \dots > b_N$

$$b_j < \frac{1}{\sqrt{N}}, \text{ for } j \in 2,\dots,N \tag{33}$$

Thus

$$\sum_{i=1}^N b_i < N \times \frac{1}{N} = 1 \tag{34}$$

which contradicts $b \in W$.

Combine the above proofs, and the fact that W is a closed and connected subset of a unit sphere, it can be concluded that x and y are the farthest vector pair in W .

In property 2.2, the set W is the set of EVS, hence $[1,0,\dots,0]^T$ and $[1/\sqrt{N},\dots,1/\sqrt{N}]^T$ are the farthest pair of EVS and the maximal value of d_{EVS} is $\|[1,0,\dots,0]^T - [1/\sqrt{N},\dots,1/\sqrt{N}]^T\|_2 = \sqrt{2-2/\sqrt{N}}$.

As $d_{EVS}(g,h)$ measures the difference between networks, alternatively, an agreement measure can be defined as a complement of EVSD,

$$\alpha_{EVS} = 1 - d_{EVS}(g,h) \tag{35}$$

Eigenvector Signature Agreement (EVSA) is the network similarity measure induced by the EVS. It represents a measure of similarity between two networks; the higher the value, the more similar the networks. It is a normalized measure and lies within the range $[0, 1]$. An illustrative example of EVSA computation can be found in File S1.

Results and Discussions

To illustrate the effectiveness of the proposed EVSA similarity score, standard test networks were used and will be given in Section 3.1. Then in Section 3.2, an application of EVSA is demonstrated with the analysis of protein-protein interaction (PPI) networks for a family of herpesvirus.

3.1 Control Test on Standard Network Models

In this section, a test based on artificially generated networks is conducted to illustrate the use of EVSA. The network models will be given in Section 3.1.1 and the results of the test can be found in Section 3.1.2. These models are chosen to conduct the algorithm test as their structure and properties are well known.

3.1.1 Network models

Four network models were chosen for testing: the Erdős Rényi random graph (ER), Barabási Albert model (BA), Geometric random graph (GEO), and Stickiness model (STICKY).

Erdős Rényi random graph (ER) A network is generated randomly without considering any geometric or probability distribution constraints. It starts with N isolated nodes and $\frac{N(N-1)}{2}$ candidate edges. Candidate edges are all possible vertex pairs for edge being attached to which can be defined as the set $\{(i,j)|i \in V, j \in V, i \neq j\}$. For each candidate edge, there is a constant probability p for an edge to be attached [19].

Barabási Albert model (BA) A scale-free network is generated through the preferential attachment scheme. Unlike the ER model, the probability of edges attachment in this model are not constant. It is directly proportional to the degree of nodes. Thus the resulting networks will reflect “the rich get richer” phenomenon. The degree distribution of a scale free network follows a power law. That is $P(k) \sim ck^\gamma$, where $P(k)$ is the population of nodes having degree k , c and γ are constants [20].

Geometric random graph (GEO) A networks is generated randomly by the following procedures. Initially, nodes are randomly distributed in an N -dimensional Euclidean space. For any node pairs having geometric distance smaller than the threshold radius r , a link will be attached among them. In this paper the three-dimensional case is considered [21].

Stickiness model (STICKY) It is a network model designed for PPI networks. By providing the degree sequence of a network, the Stickiness model can be used to generate a set of networks having the same degree sequence. There are two main assumptions, i) the higher degree nodes have more reaction domain, i.e. these nodes can interact more frequently, ii) a stickiness index is defined; where a node pair both have a higher stickiness index, they are more willing to interact with each other. The stickiness index of nodes helps to control the expected degree sequence of the generated network [22]. The Stickiness model is designed to mimic a network based on the degree sequence, which is only used in the test among standard models; and in the study of herpesvirus PPI networks (Section 3.2), but not in the performance analysis (Section 3.2.2).

3.1.2 Control Test Results. The control test was performed by first generating a reference network from each model, parameters were adjusted such that the size and average degree were 500 and approximately 10 respectively. Then perturbed the reference network by different ways: (a) randomly attaching k edges on the reference network, where $k = \lfloor \phi E \rfloor$, E is the total number of edges in the reference network and $\phi \in [0, 1]$ is an adjustable parameter for testing purpose (see Table 1); (b) randomly selecting ϕ of the nodes in the reference network, replacing the interconnection of the selected nodes by a ER network; (c), (d) and (e) are similar to (b), but the injected network are GEO3D type, BA type and STICKY type respectively. EVSA between the reference networks and perturbed networks were then

computed. The control test was repeated 50 times for each case and the mean EVSA were summarized in Table 1.

While the reference network was being perturbed by random attachment, most of the topology remained the same, thus in most of the cases the mean EVSA values were high. Yet in the case of GEO3D, the topology of reference network follows a geometric constrains, random attachment of edges violated this constrain and caused a large difference in topology. According to the results, randomly attaching 50% extra edges caused the mean EVSA score changed from 1 to 0.5323. On the other hand, in tests (b) to (e), the EVSA scores were found to be close among different types of injection with the same reference network and ϕ value. For instance, injecting a GEO3D network and BA network on a ER network with $\phi = 0.5$ caused their mean EVSA values dropped from 1 to 0.9597 and 0.9609 respectively. This indicated that even the interconnection between part of the nodes were replaced by various types of network, the similarity between the original network and the perturbed network can still be reflected by their high EVSA.

3.2 Analysis on Protein-Protein Interaction Networks

In this section, five herpesviral PPI networks are analyzed using EVSA. The employed data set is described in Section 3.2.1, and the results can be found in Section 3.2.2.

3.2.1 Protein-Protein Interaction Networks. The PPI network is a network that consists of proteins and their interactions within a single organism, for example baker's yeast and human. In the PPI network a protein is represented in the form of nodes. For every pair of proteins having interaction, a link will be attached in between the corresponding nodes. Here, five herpesvirus PPI networks were chosen for the evaluation, namely Epstein-Barr virus (EBV), herpes simplex virus (HSV), Kaposi's sarcoma-associated herpesvirus (KSHV), murine cytomegalovirus (mCMV)

Table 1. This table summarized the EVSA values obtained from a series of control tests.

| Type of Reference Network | ϕ | (a) | (b) | (c) | (d) | (e) |
|---------------------------|--------|--------|--------|--------|--------|--------|
| ER | 0 | 1 | 1 | 1 | 1 | 1 |
| | 0.1 | 0.9814 | 0.9937 | 0.9935 | 0.9932 | 0.9934 |
| | 0.2 | 0.9716 | 0.9856 | 0.9869 | 0.9865 | 0.9873 |
| | 0.3 | 0.9607 | 0.9769 | 0.9778 | 0.9779 | 0.9770 |
| | 0.4 | 0.9513 | 0.9659 | 0.9683 | 0.9674 | 0.9669 |
| | 0.5 | 0.9440 | 0.9598 | 0.9597 | 0.9609 | 0.9582 |
| GEO3D | 0 | 1 | 1 | 1 | 1 | 1 |
| | 0.1 | 0.8061 | 0.9873 | 0.9683 | 0.9804 | 0.9693 |
| | 0.2 | 0.6914 | 0.9720 | 0.9410 | 0.9458 | 0.9460 |
| | 0.3 | 0.6213 | 0.9533 | 0.8760 | 0.9129 | 0.9156 |
| | 0.4 | 0.5705 | 0.9325 | 0.8477 | 0.8367 | 0.8841 |
| | 0.5 | 0.5323 | 0.8926 | 0.7994 | 0.8123 | 0.8262 |
| BA | 0 | 1 | 1 | 1 | 1 | 1 |
| | 0.1 | 0.9786 | 0.9898 | 0.9892 | 0.9900 | 0.9888 |
| | 0.2 | 0.9607 | 0.9735 | 0.9785 | 0.9732 | 0.9751 |
| | 0.3 | 0.9431 | 0.9616 | 0.9603 | 0.9520 | 0.9548 |
| | 0.4 | 0.9258 | 0.9466 | 0.9412 | 0.9279 | 0.9340 |
| | 0.5 | 0.9087 | 0.9304 | 0.9142 | 0.9120 | 0.9146 |

The first column indicates the network class of the reference network, the second column indicates the ϕ values in the control tests. Column (a) to (e) are the mean EVSA value obtained from 50 times of the corresponding test. (a) is the random edge attachment test, (b) is the ER injection test, (c) is the GEO3D injection test, (d) is the BA injection test and (e) is the STICKY injection test.

doi:10.1371/journal.pone.0109383.t001

Table 2. Summary Statistics of Yeast and Human PPI Network obtained from Rito et al.

| Name | # Nodes | # Edges | Graph Density | Average Degree | Experiment Type | Organism | Reference |
|-------|---------|---------|---------------|----------------|---------------------|---------------|--------------------------|
| YIC | 796 | 841 | 0.0027 | 2.11 | Yeast two-hybrid | S. Cerevisiae | Ito et al. (2000) |
| YHS | 988 | 2455 | 0.0050 | 4.97 | TAP-MS | S. Cerevisiae | Von Mering et al. (2002) |
| HSHS | 1705 | 3186 | 0.0022 | 3.74 | Yeast two-hybrid | Homo Sapiens | Stelzl et al. (2005) |
| BG MS | 1923 | 3866 | 0.0021 | 4.02 | Affinity Capture-MS | Homo Sapiens | BIOGRID (filtered) |

doi:10.1371/journal.pone.0109383.t002

and varicella-zoster virus (VZV). These five herpesviral PPI networks were collected by Peter Uetz et al. [23,24].

The following is an illustrative analysis on several PPI networks. The summary statistics of yeast and human PPI networks including graph density, are shown in Table 2. This is obtained from a study on GDDA [25]. According to that study, when the graph density is low, GDDA will suffer from a volatility issue.

Here a similar analysis is conducted on five herpesvirus PPI networks: Epstein Barr virus (EBV), Herpes simplex virus (HSV), Kaposi's sarcoma-associated herpesvirus (KSHV), murine cytomegalovirus (mCMV) and varicella-zoster virus (VZV). The summary statistics can be found in Table 3. In the herpesvirus case, the graph density is relatively higher (0.06 to 0.12) than the yeast-human case (0.0007 to 0.005), which indicates that the low graph density property is not consistent in all PPI networks. This inconsistency may be caused by the definition of graph density.

$$\rho = \frac{2e}{N(N-1)} \quad (36)$$

Graph density is sensitive to network size since $\rho \sim O(N^{-2})$, thus there exists an inconsistency between a small PPI network (e.g. herpesvirus) and a large PPI network (e.g. yeast). In this paper, instead of graph density, the average degree is being considered. The average degree is defined as

$$deg_{avg} = \frac{2e}{N} \quad (37)$$

As $deg_{avg} = O(N^{-1})$, which is less sensitive to network size and hence is a more suitable candidate of changing variable in the performance evaluation for network similarity measures. This observation can be supported by the summary statistic as shown in Table 2 and 3; where average degree in yeast and human PPI network is around 2 to 5, in herpesvirus network it is about 4 to 7. It shows that average degree of node is more consistent than graph density among these three kinds of PPI networks. Note that by adjusting the average degree and network size, different ranges of graph density can also be covered.

3.2.2 Results on Protein-Protein Interaction Networks. The procedure can be summarized as follows: first pick one of the herpesvirus PPI networks and compute its total number of edges, for each of the four models (ER, BA, GEO3D, STICKY), generate 50 candidate networks where the parameters are adjusted so that they have approximately the same number of edges as the herpesvirus networks. Then the EVSA score between the selected herpesvirus network and each of its candidate networks are computed, the EVSA scores are then averaged for each model. This average EVSA score is considered as the similarity score between the query network (e.g. EBV) and the testing model (e.g. ER). The process is repeated until all herpesvirus networks have been tested.

Figure 1 shows the EVSA score of EBV, HSV, KSHV, mCMV and VZV matching with ER, GEO3D, SF and STICKY respectively. The EVSA scores between the STICKY model and the five herpesvirus networks are clearly higher than the other models. ER, GEO3D and BA have average EVSA scores around 0.8 and STICKY has average EVSA scores around 0.9. Since the STICKY model is distinct from the other three models in the matching test of herpesvirus PPI networks; we can observe that considering only ER, GEO3D, BA and STICKY models as candidates, STICKY is the closest model with respect to the

Table 3. Summary Statistics of HSV, VZV, KSPV, EBV, and mCMV PPI Network.

| Name | # Nodes | # Edges | Graph Density | Average Degree | Experiment Type | Organism | Reference |
|------|---------|---------|---------------|----------------|------------------|---------------------------------------|----------------------|
| HSV | 48 | 100 | 0.0886 | 4.167 | Yeast two-hybrid | Herpes simplex virus | Fossum et al. (2009) |
| VZV | 55 | 159 | 0.1070 | 5.782 | Yeast two-hybrid | Varicella zoster virus | Uetz et al. (2006) |
| KSPV | 50 | 115 | 0.0938 | 4.6 | Yeast two-hybrid | Kaposi sarcoma-associated herpesvirus | Uetz et al. (2006) |
| EBV | 60 | 208 | 0.1175 | 6.933 | Yeast two-hybrid | Epstein - Barr Virus | Fossum et al. (2009) |
| mCMV | 111 | 393 | 0.0643 | 7.081 | Yeast two-hybrid | Murine cytomegalovirus | Fossum et al. (2009) |

doi:10.1371/journal.pone.0109383.t003

herpesvirus family. This can also be interpreted that given only the degree sequence as information, one can reconstruct the PPI network of herpesvirus with similar topology using the stickiness model.

A similar analysis using GDDA was also conducted on the same five herpesviral PPI networks and yielded the same conclusion, STICKY is the best-fitting model of herpesvirus [26]. However, compared to the GDDA approach, the EVSA score is relatively stable among five herpesvirus PPI networks and the separation of EVSA scores between the STICKY model and the other network models is more apparent. This demonstrates that our results reinforce the observation of Kuchaiev et al. In Section 3.2.2, we will show that EVSA has higher stability and better classification performance.

Performance Evaluation

Finally, the performance of network classification using EVSA is given and compared with another signature based network classification techniques: GDDA. In Section 4.1, the design of the testing is introduced. Volatility and classification performance of these two similarity score systems are compared in Sections 4.2 and 4.3 respectively.

4.1 Designs of Experiment

In order to illustrate the performance of different similarity score systems, models introduced in Section 3.1.1 was employed to generate networks for testing purposes. The experiment was conducted as follows.

Given two network models, for example ER model and BA model: in a ER-BA comparison, networks randomly generated from ER model using parameter set $\{N_j, \theta_j^{ER}\}$ was considered as query network (G_Q^{ER}), where N_j is the network size and θ_j^{ER} is the rest of ER model parameters. Similarly, 50 candidate networks $\{G_1^{BA}, \dots, G_{50}^{BA}\}$ with same size N_j was randomly generated from BA model. The parameters θ_j^{BA} were adjusted such that the resulting candidate networks had approximately the same edge number to the one in G_Q^{ER} .

The GDDA scores and EVSA scores between the query network and each of the candidate networks (i.e. $GDDA(G_Q^{ER}, G_k^{BA})$ and $\alpha_{EVS}(G_Q^{ER}, G_k^{BA})$ for $k=1, \dots, 50$) can then be computed. The process was repeated for several parameter sets $\{N_i, \theta_i^{ER}\}$, until all the interested $\{N_i, \theta_i^{ER}\}$ were considered. In this paper, the interested networks were limited to those with size 50, 100, 500, 1000, 2000 nodes and average degree 2,3,...,10. According to Section 3.2.1, these values cover most of the PPI networks of human, yeast and herpesviruses.

Comparisons between models can be separated into two classes; the match and the mismatch set comparisons. Match set comparisons are comparisons between networks generated from the same model, for instance, ER-ER comparison. Mismatch set comparisons are comparisons of networks generated across different models, for instance, ER-BA comparison. The score distribution of these two classes of comparison were used to illustrate the classification performance in Section 4.3.

4.2 Volatility of EVSA and GDDA

The stability of similarity score is an important issue as it directly affects the confidence of classification and the reliability of the scores. It can be measured as the standard deviation of a score among similar comparisons. An ideal similarity score should be non-volatile. Here our proposed similarity score EVSA is

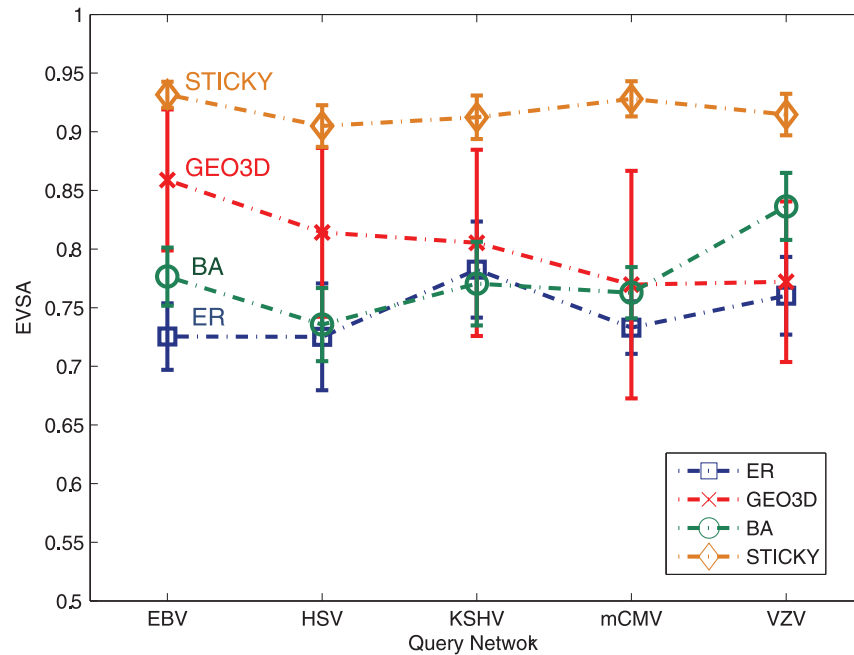


Figure 1. EVSA values of pairwise comparisons between PPI networks of EBV, HSV, KSHV, mCMV and VZV and network generated from ER, GEO3D, BA, STICKY models. The EVSA scores are averaged over 50 simulations and the error bar represents one standard deviation of the EVSA score.

doi:10.1371/journal.pone.0109383.g001

compared with GDDA in terms of volatility. The EVSA scores were computed using the algorithm mentioned in previous sections. GDDA scores were computed using GraphCrunch 2.

Table 4 shows the standard deviation of EVSA scores and GDDA scores in ER-ER, BA-BA and GEO3D-GEO3D comparisons with different average degrees respectively. According to Table 4, in most of the cases EVSA has a lower deviation as compare to GDDA. However, exceptions are found in low density cases and these exceptions are caused by the volatility of the model itself. In a recent study of network comparisons [27], topologies of low density or low average degree graphs are considered as highly volatile. A sensitive similarity measures could reflect this fact in terms of high deviation. This explained the relatively higher deviation of EVSA on lower average degree networks. For instance, in ER-ER comparison among networks with an average degree of 2, the standard deviation of EVSA is 0.0703 which is higher than that of GDDA (0.0565). On the other hand, in a higher average degree graph, the EVSA yields a relatively lower deviation which reflects the stability of the measure. For instance, in BA-BA comparison among networks with an average degree of 10, the standard deviation of EVSA is 0.0326 which is much lower than GDDA's (0.0737). Thus from this experiment, the higher sensitivity and robustness of EVSA is demonstrated.

4.3 Classification Performance of EVSA and GDDA

Besides the volatility, the classification power of EVSA and GDDA is also an interesting aspect. The following is a test designed to reflect the classification power of a score. The basic idea of this test is to compare the distribution of scores in two cases, (i) networks generated from the same model and (ii) networks generated from different models.

In this experiment, networks were generated using ER, BA and GEO3D models. At the beginning of the test, a set of query networks was generated using different parameters through

different models. For each of the networks in the query set, a number of candidate networks were generated using all three models. The parameters of the network model were chosen to generate networks with the same vertex number and approximately the same edge number. So the networks have approximately equal average node degree and graph density. With this set of candidate networks a set of GDDA and EVSA scores can be computed between each query network and their candidate networks. Here the GDDA scores were computed using the network analysis application GraphCrunch 2 [26].

The GDDA and EVSA scores were further classified into agreement scores of matching and mismatching sets respectively. Matching and mismatching agreements are the set of agreement scores where query networks and candidate networks are generated from the same and different model types respectively.

The analysis results are summarized in Figures 2 and 3 in the form of a grey scale heat map. It shows the average GDDA and average EVSA in different parameter settings. The x-axis of the subplot represents the network size/vertex number; the y-axis represents the average degree of nodes. According to Figure 3, for GDDA, the difference between match-model comparisons (ER-ER, BA-BA, GEO3D-GEO3D) and mismatch-model comparisons (ER-BA, ER-GEO3D, BA-ER, etc) is not significant. While in the case of EVSA (Figure 2), notable difference is observed.

This reflects that the average EVSA scores among networks generated from the same model and those from different models have notable differences. It indicates that EVSA score can provide a clearer difference between the matching cases and the mismatching cases, or that the fuzziness and the mentioned difficulty on classification can be reduced.

To have a deeper understanding of the classification power of GDDA and EVSA, all the scores were being sampled and analyzed in terms of their distributions. The sampled data are illustrated in Figure 4 and 5 in histogram form. In EVSA, two sets of distributions can be found to be more divergent, which indicates

Table 4. Standard deviation of EVSA, GDDA in same model comparison over various average degrees.

| Average Degree | Standard Deviation | | | | | |
|----------------|--------------------|---------------|---------------|---------------|---------------|--------|
| | ER-ER | | BA-BA | | GEO3D-GEO3D | |
| | EVSA | GDDA | EVSA | GDDA | EVSA | GDDA |
| 2 | 0.0703 | 0.0565 | 0.0688 | 0.0649 | 0.0309 | 0.0460 |
| 3 | 0.0481 | 0.0726 | 0.0608 | 0.0731 | 0.0218 | 0.0332 |
| 4 | 0.0266 | 0.0467 | 0.0563 | 0.0539 | 0.0362 | 0.0502 |
| 5 | 0.0369 | 0.0334 | 0.0521 | 0.0518 | 0.0318 | 0.0332 |
| 6 | 0.0282 | 0.0485 | 0.0523 | 0.0567 | 0.0182 | 0.0428 |
| 7 | 0.0206 | 0.0526 | 0.0392 | 0.0499 | 0.0288 | 0.0766 |
| 8 | 0.0181 | 0.0484 | 0.0332 | 0.0605 | 0.0362 | 0.0464 |
| 9 | 0.0190 | 0.0505 | 0.0501 | 0.0671 | 0.0218 | 0.0401 |
| 10 | 0.0173 | 0.0558 | 0.0326 | 0.0737 | 0.0309 | 0.0618 |

doi:10.1371/journal.pone.0109383.t004

that it provides a higher confidence for classification. In the GDDA case, the score distribution of matching models and mismatching models highly overlap when using GEO3D and BA networks as the query models. These overlapping regions are the “twilight zone” of the classification. The existence of such a region reduces the classification confidence and introduces fuzziness of classification.

To compare the divergence of matching and mismatching cases in GDDA and EVSA, the Jaccard distance is employed [28]. The Jaccard distance quantifies the divergence between two sets of distributions within a range from 0 to 1. A higher Jaccard distance

indicates that the two distributions are more divergent and vice versa. Definition of Jaccard distance can be found in File S1.

Table 5 summarizes the Jaccard distance between matching and mismatching sets of GDDA and EVSA in three cases respectively: ER, GEO3D and BA type query networks. In GDDA, using ER network as the query network can yield a good Jaccard distance in classification (0.9149). While in cases using GEO3D and BA network as the query network, the classification power varies over a large range in terms of Jaccard distance (0.3060 and 0.7477). A good performance in a single case but less desire in other cases may lead to fuzzy inference results in

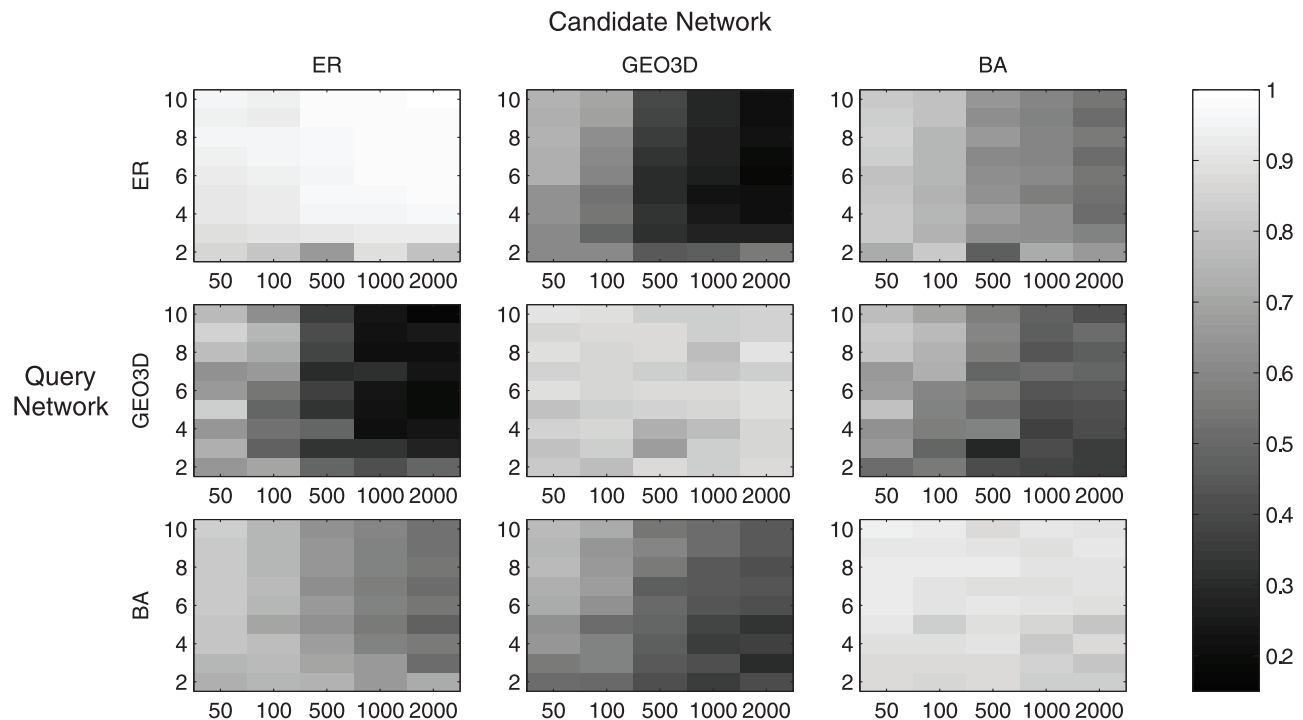


Figure 2. Heat map of average EVSA score in various comparisons. Each subplot represents the heat map of average EVSA score of a single type comparison. For instance, the bottom left subplot is the comparison of Scale-free (SF) network versus Erdos Renyi (ER) network, SF network is the Query Network and ER network is the candidate network. In each subplot, the y-axis represents the average degree, x-axis represents the network size (vertex number) the grey level represents the average EVSA score.
doi:10.1371/journal.pone.0109383.g002

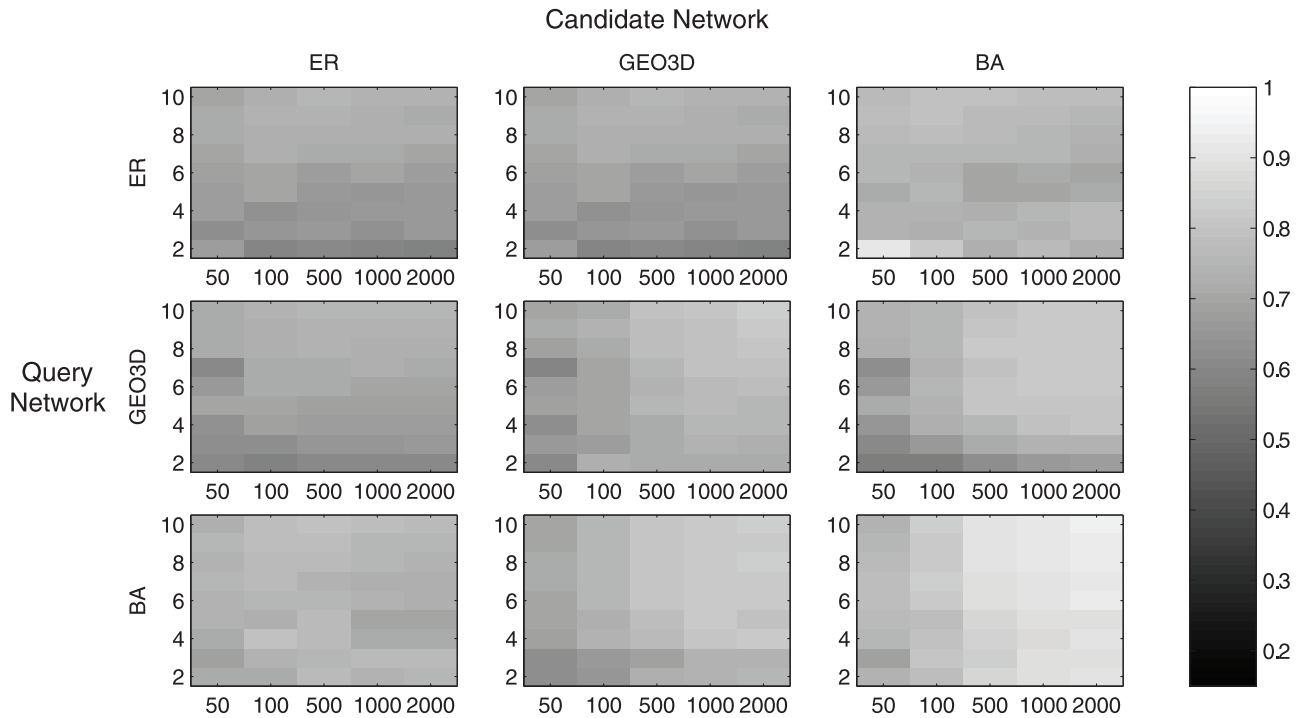


Figure 3. Heat map of average GDDA score in various comparisons. Each subplot represents the heat map of average GDDA score of a single type comparison. For instance, the bottom left subplot is the comparison of Scale-free (SF) network versus Erdos Renyi (ER) network, SF network is the Query Network and ER network is the candidate network. In each subplot, the y-axis represents the average degree, x-axis represents the network size (vertex number) the grey level represents the average.
doi:10.1371/journal.pone.0109383.g003

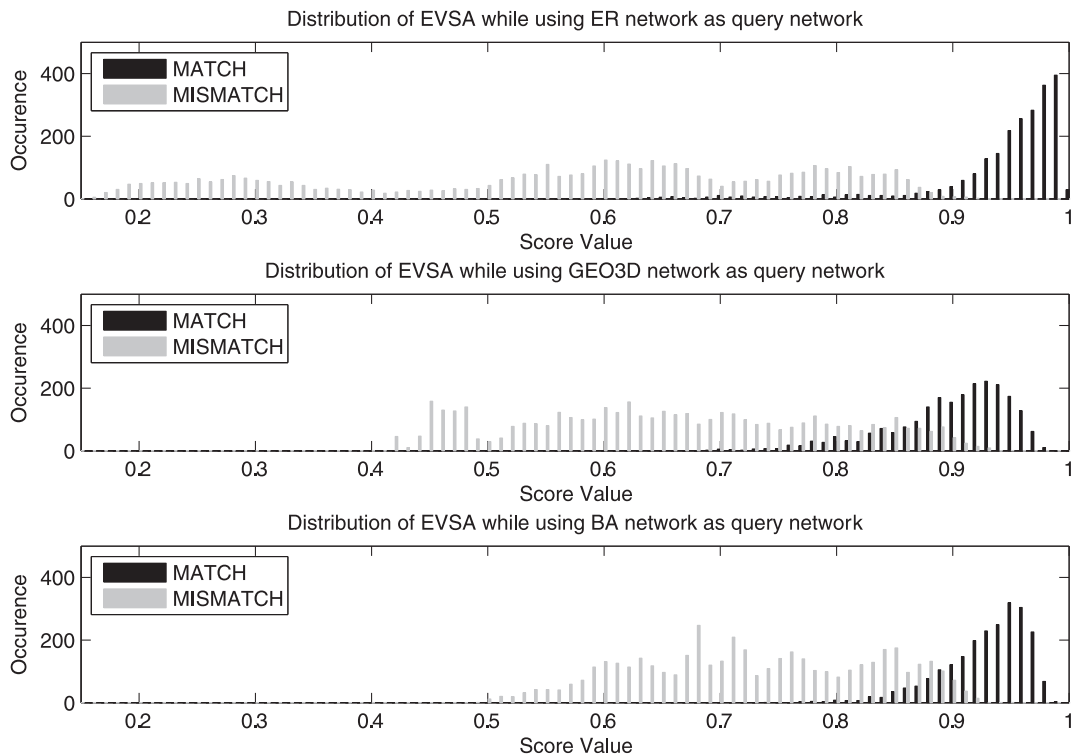


Figure 4. Sampled population of EVSA score. From top to bottom are a) ER network, b) GEO3D network, c) BA network as the query network used respectively.
doi:10.1371/journal.pone.0109383.g004

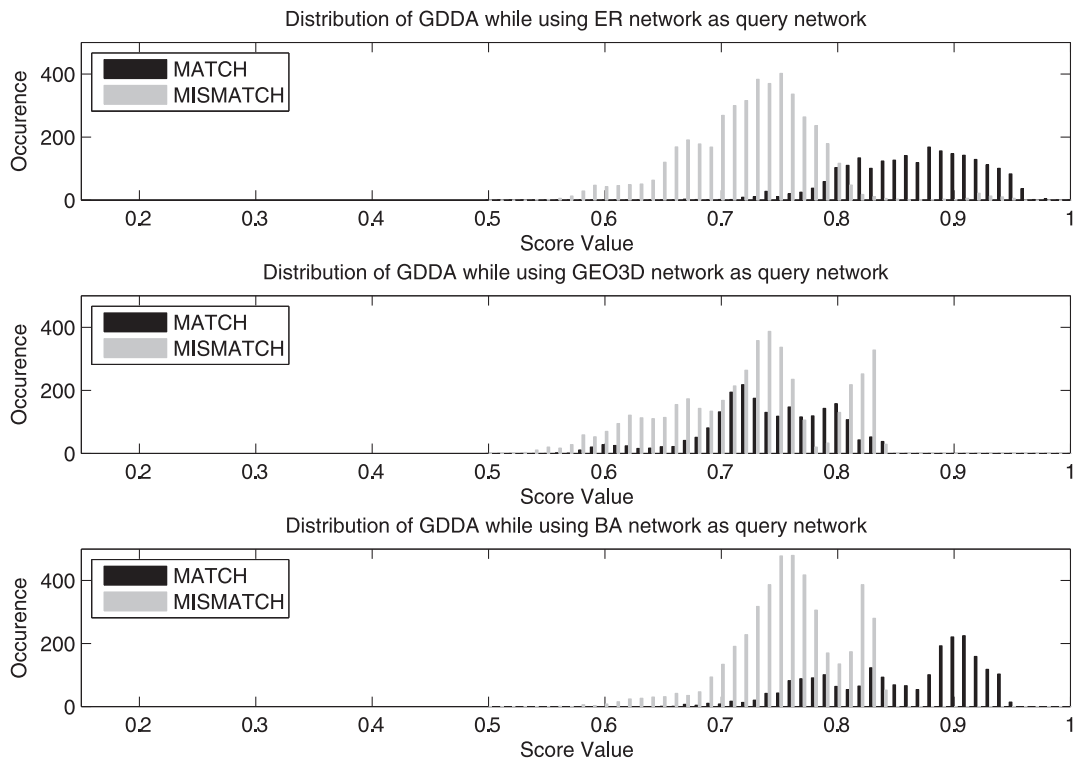


Figure 5. Sampled population of GDDA score. From top to bottom are a) ER network, b) GEO3D network, c) BA network as the query network used respectively.
doi:10.1371/journal.pone.0109383.g005

classifying practical networks. In EVSA, all three types of query networks can yield a higher and more stable Jaccard distance around 0.9.

On the other hand we also evaluated the classification performance of GDDA and EVSA via applying them on a support vector machine (SVM) classifier as kernel values [29,30]. The SVM model classifies whether a network belongs or not to a specific class. The performances of the models are evaluated via a 5-fold cross validation and the results are summarized in Table 6. According to the results, model using EVSA as kernel value is relatively better than the one using GDDA in terms of accuracy, especially while classifying BA networks.

Conclusions

In this paper the Eigenvector Signature is proposed. With this signature, the original matrix alignment problem in network characterization can be transformed into a vector alignment

problem. Consequently the computational complexity can be drastically reduced from $O(N^4)$ to $O(N \log N)$. In addition, an agreement measure - Eigenvector Signature Agreement (EVSA) is designed to quantify the similarity between networks.

Experimental results have shown that EVSA has a stable classification behaviour among various settings of different network models, including ER random graph, BA scale free network and geometric 3D random network. An application of EVSA on classifying herpesvirus PPI networks had also been conducted. The results are consistent with the previous studies, with much faster speed. Furthermore, performance analysis between EVSA and another signature based graph similarity measure GDDA had also been conducted. Results show that EVSA can achieve higher stability and better classification performance. Moreover, since EVSA quantifies network similarity, it can also be considered as a graph kernel. Hence kernel-based learning algorithms can also be applied.

Table 5. The Jaccard Distance of GDDA and EVSA between matching and mismatching network sets.

| Query Network | Jaccard Distance | |
|---------------|------------------|--------|
| | EVSA | GDDA |
| ER | 0.9942 | 0.9149 |
| GEO3D | 0.9149 | 0.3060 |
| BA | 0.9455 | 0.7477 |

doi:10.1371/journal.pone.0109383.t005

Table 6. The accuracy from 5-fold cross validation of SVM using EVSA and GDDA as kernel.

| Class 1 | Class 2 | Accuracy | |
|---------|-----------|---------------|-------------|
| | | EVSA kernel | GDDA kernel |
| ER | Not ER | 81.48% | 77.78% |
| GEO3D | Not GEO3D | 92.59% | 81.48% |
| BA | Not BA | 96.30% | 66.67% |

doi:10.1371/journal.pone.0109383.t006

Supporting Information

File S1 Supporting information. Definition S1: Jaccard Index and Jaccard Distance. Computation S1: Example of EVSA Computation. (PDF)

Acknowledgments

The authors would like to thank Peter Utez and Even Fossum who had kindly provided their herpesvirus PPI dataset and explained in details. The

authors would also like to thank Robin Sarah Bradbeer and Anita Soley for their advices.

Author Contributions

Conceived and designed the experiments: BL LY KK GY. Performed the experiments: BL LY CZ. Analyzed the data: BL LY CZ KK GY. Contributed reagents/materials/analysis tools: BL LY CZ KK GY. Wrote the paper: BL LY CZ KK GY.

References

- Vishwanathan S, Schraudolph NN, Kondor R, Borgwardt KM (2010) Graph kernels. *The Journal of Machine Learning Research* 11: 1201–1242.
- Brandes U, Erlebach T (2005) *Network analysis: methodological foundations*, volume 3418. Springer.
- Takigawa I, Mamitsuka H (2013) Graph mining: procedure, application to drug discovery and recent advances. *Drug discovery today* 18: 50–57.
- Wegner JK, Sterling A, Guha R, Bender A, Faulon JL, et al. (2012) Cheminformatics. *Communications of the ACM* 55: 65–75.
- Umeyama S (1988) An eigendecomposition approach to weighted graph matching problems. *Pattern Analysis and Machine Intelligence, IEEE Transactions on* 10: 695–703.
- Singh R, Xu J, Berger B (2008) Global alignment of multiple protein interaction networks with application to functional orthology detection. *Proceedings of the National Academy of Sciences* 105: 12763–12768.
- Li Z, Zhang S, Wang Y, Zhang XS, Chen L (2007) Alignment of molecular networks by integer quadratic programming. *Bioinformatics* 23: 1631–1639.
- Milo R, Shen-Orr S, Itzkovitz S, Kashtan N, Chklovskii D, et al. (2002) Network motifs: simple building blocks of complex networks. *Science Signaling* 298: 824.
- Pržulj N, Corneil DG, Jurisica I (2004) Modeling interactome: scale-free or geometric? *Bioinformatics* 20: 3508–3515.
- Milenković T, Pržulj N (2008) Uncovering biological network function via graphlet degree signatures. *Cancer informatics* 6: 257.
- Milenković T, Ng WL, Hayes W, Pržulj N (2010) Optimal network alignment with graphlet degree vectors. *Cancer informatics* 9: 121.
- Pržulj N (2007) Biological network comparison using graphlet degree distribution. *Bioinformatics* 23: e177–e183.
- Papadopoulos AN, Manolopoulos Y (1999) Structure-based similarity search with graph histograms. In: *Database and Expert Systems Applications, 1999. Proceedings. Tenth International Workshop on. IEEE*, pp. 174–178.
- Chartrand G, Kubicki G, Schultz M (1998) Graph similarity and distance in graphs. *Aequationes Mathematicae* 55: 129–145.
- Bunke H, Shearer K (1998) A graph distance metric based on the maximal common subgraph. *Pattern recognition letters* 19: 255–259.
- Blondel VD, Gajardo A, Heymans M, Senellart P, Van Dooren P (2004) A measure of similarity between graph vertices: Applications to synonym extraction and web searching. *SIAM review* 46: 647–666.
- Mises R, Pollaczek-Geiringer H (1929) Praktische verfahren der gleichungsauflosung. *ZAMM-Journal of Applied Mathematics and Mechanics/Zeitschrift für Angewandte Mathematik und Mechanik* 9: 58–77.
- Hardy GH, Littlewood JE, Pólya G (1952) *Inequalities*. Cambridge university press.
- Erdős P, Rényi A (1959) On random graphs. *Publicationes Mathematicae Debrecen* 6: 290–297.
- Barabási AL, Albert R (1999) Emergence of scaling in random networks. *science* 286: 509–512.
- Penrose M (2003) *Random geometric graphs*, volume 5. Oxford University Press Oxford.
- Pržulj N, Higham DJ (2006) Modelling protein–protein interaction networks via a stickiness index. *Journal of the Royal Society Interface* 3: 711–716.
- Uetz P, Dong YA, Zeretzke C, Atzler C, Baiker A, et al. (2006) Herpesviral protein networks and their interaction with the human proteome. *Science* 311: 239–242.
- Fossum E, Friedel CC, Rajagopala SV, Titz B, Baiker A, et al. (2009) Evolutionarily conserved herpesviral protein interaction networks. *PLoS pathogens* 5: e1000570.
- Rito T, Wang Z, Deane CM, Reinert G (2010) How threshold behaviour affects the use of subgraphs for network comparison. *Bioinformatics* 26: i611–i617.
- Kuchaiev O, Stevanović A, Hayes W, Pržulj N (2011) Graphcrunch 2: Software tool for network modeling, alignment and clustering. *BMC bioinformatics* 12: 24.
- Hayes W, Sun K, Pržulj N (2013) Graphlet-based measures are suitable for biological network comparison. *Bioinformatics* 29: 483–491.
- Cha SH (2007) Comprehensive survey on distance/similarity measures between probability density functions. *International Journal of Mathematical Models and Methods in Applied Science* 1: 1.
- Cortes C, Vapnik V (1995) Support-vector networks. *Machine learning* 20: 273–297.
- Chang CC, Lin CJ (2011) LIBSVM: A library for support vector machines. *ACM Transactions on Intelligent Systems and Technology* 2: 27:1–27:27.